SEISMIC BEHAVIOUR OF A STRUCTURAL CLAY TILE INFILL WALL

J. Therrien-Truchon[1], P. Paultre[2] and J. Proulx[3]
[1] Junior engineer, Julie.Therrien-Truchon@usherbrooke.ca
[2] Professor, Department of Civil Engineering, University of Sherbrooke, Sherbrooke, QC, J1K 2R1, Canada, Patrick.Paultre@usherbrooke.ca
[3] Professor, Department of Civil Engineering, University of Sherbrooke, Sherbrooke, QC, J1K 2R1, Canada, Jean.Proulx@usherbrooke.ca.

ABSTRACT
A significant portion of unreinforced masonry (URM) school buildings in Central Quebec were built in the 1950s and 60s. Construction types include steel, concrete and wood frames with URM used as infill on the perimeter as well as non-structural partition walls. A recent inventory survey carried out on buildings for which the outer brick walls were being repaired or replaced showed that the peripheral infill material was often unreinforced hollow structural clay tiles (terracotta). This material, now difficult to find in Canada, was widely used at the time as infill to steel or concrete frames. As school buildings are designated as priority buildings, the evaluation of their earthquake resistance requires a reliable knowledge of their dynamic behavior. This paper presents a research project that was developed to characterize structural clay tiles and typical walls built with this material when subjected to seismic forces. Cyclic tests were carried out on a typical first-floor outer wall specimen that could have been located in a typical 1950s school building, based on findings from a survey of more than 55 school buildings. The structural clay tile wall specimen measured approximately 3x3 m enclosed by a steel frame. Characterization tests were also carried out on single tiles as well as small tiles assemblies to obtain information on compression strength, elastic modulus and Poisson's ratio. Results are presented and discussed for key parameters (stiffness, load-bearing capacity, deformation and energy dissipation). Experimental results were compared with numerical predictions obtained with the SeismoStruct nonlinear program, using the masonry element based on the equivalent strut concept.

KEYWORDS: seismic behaviour, unreinforced masonry, in-plane cyclic test, infill wall, structural clay tile, school buildings

INTRODUCTION
The province of Quebec, Canada, is located in a moderate seismic zone. The city of Montreal, for example, has the second highest urban seismic risk in Canada, and the Charlevoix region has PGA values up to 1.10 g. A large portion of the schools built in the 1950-1970 period includes unreinforced masonry (URM) either as infill material on the perimeter walls, or as non-structural partition walls. URM is now recognized as being vulnerable to earthquakes and its structural use is prohibited in building codes. This paper presents a research project, part of the Canadian Seismic Research Network (CSRN) [1], to characterize the dynamic behavior of a particular URM configuration that is widely used in Quebec, as found in a survey of 55 school buildings.

Experimental masonry research has been going on for more than fifty years, but the experimental results are rarely analysed with the viewpoint of seismic performance. There is also lack of experimental data specific to construction types such as those encountered in Quebec.

One of the widely used configurations involved structural clay tiles (terracotta) used as infill in the perimeter walls in many school buildings. These tiles were individually characterized and in-plane cyclic tests were carried out on a typical wall that would be located in a steel-frame school building. The experimental setup and procedures are presented, as well as key results related to the dynamic behavior of the URM wall (stiffness, load-bearing capacity, deformation and energy dissipation). A numerical correlation study is also presented. A complete description of the project can be found in reference [2].

CONSTRUCTION TYPES

A survey of more than 55 buildings was recently carried out in school board located in central Quebec [3], where the majority of buildings were constructed before modern seismic codes. Buildings were categorized according to their main structure type, exterior wall type, infill material, number of floors and construction year. The survey showed that, for the most part, the construction types consisted of concrete or steel infilled frames and light wood frames, mostly built between 1950 and 1970. Buildings were usually covered by a brick veneer with a 200 mm thick infill perimeter wall of structural clay tile (terracotta) or concrete unit. Large units were preferred as a filling material.

Figure 1 shows a typical school building with structural clay tile used as infill to steel frames. In this case, the exterior brick cladding was removed for repairs and the infill walls are apparent. These URM walls were poorly built and clearly intended as simple filling elements. Deficiencies such as a lack of mortar in the joints and the use of grout and brick to fill the web of steel beams are observed.

(a) **(b)**

Figure 1: (a) School building with structural clay tile infilled steel frames; (b) Structural clay infills in roof space of typical school building.

Although considered as a non-structural element, infills increase the lateral stiffness of the building and as a result decrease its fundamental period, resulting in underestimated seismic loads. There are, however, few reported experimental studies on structural clay tile infill walls. As this type of infill is widely used in several Quebec school boards, a research program was developed to characterize its dynamic behavior.

EXPERIMENTAL STRUCTURAL CLAY WALL SPECIMEN

Cyclic tests were carried out on a structural clay tile URM infill wall in a 2.94 m wide by 3.15 m high steel frame (Figure 2). The steel frame consisted of W310x39 columns and a W310x60 beam. Columns were welded to a double steel plate system fixed to the laboratory concrete slab. The infill wall was made of structural clay tile units with a type N mortar (1 part of Portland cement, 1 part of lime and 6 parts of sand), typical of 1950s construction in Quebec.

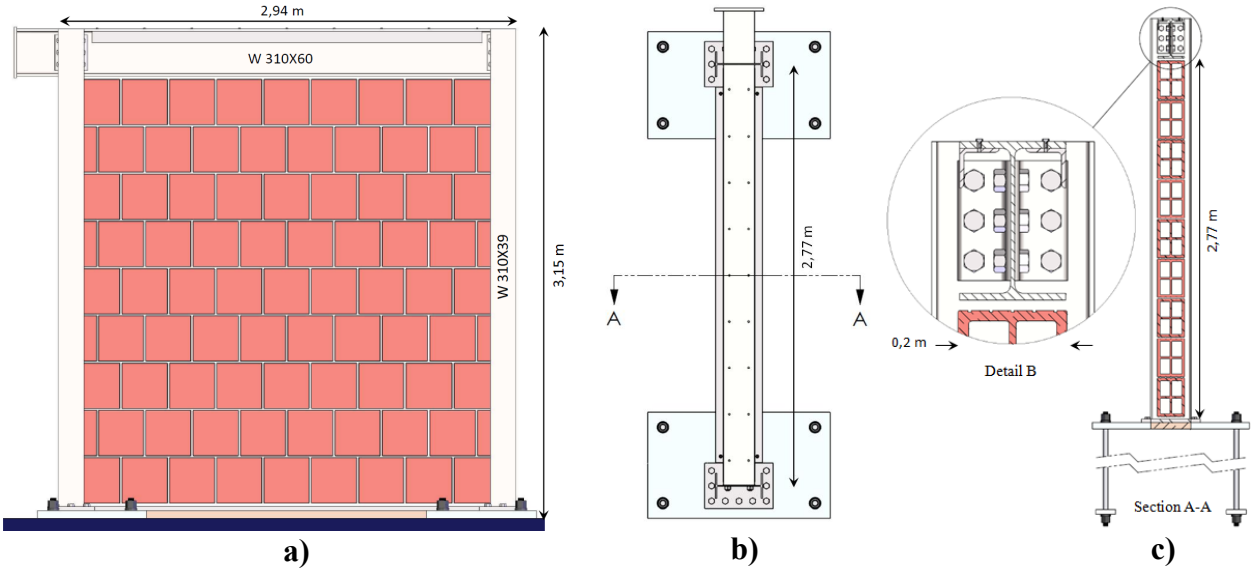

Figure 2: Experimental specimen: a) elevation; b) plan view; c) section.

The URM wall measured 2.77 x 2.77 x 0.2 m, and was centered inside the steel frame. Masonry units were laid in side construction, i.e. with cores in the horizontal direction, using 10 mm mortar joints. The structural clay tiles (which are no longer available in Canada) had nominal dimensions of 200 x 300 x 300 mm, Figure 3. An experienced mason was hired to construct the wall specimen using 1950s practice.

A reaction wall was used to apply a cyclic lateral load with a 500 kN actuator. Steel guides were added on each side of the beam for lateral out-of-plane support. A quasi-static in-plane cyclic load was applied on the specimen. The loading was displacement controlled and each cycle repeated twice. The experimental setup is illustrated in Figure 4.

CHARACTERIZATION OF THE STRUCTURAL CLAY TILES

Key properties (elastic modulus, Poisson's ratio, etc.) of the structural clay tiles were obtained by characterization tests prior to the large-scale cyclic tests. Four types of specimens were used for compressive tests in accordance with ASTM C109, C67, C1314, E519 standards [4-7]: mortar

cubes, individual tiles (T), prisms of two tiles (P) and 4x4 tiles prisms tested in a diagonal setup (D). Figure 5 shows the diagonal compression test setup and the clamping system for the 4x4 tile prisms. The loading surfaces were prepared with Flowstone, a gypsum mortar that met the requirements of ASTM C1552 capping standard [8].

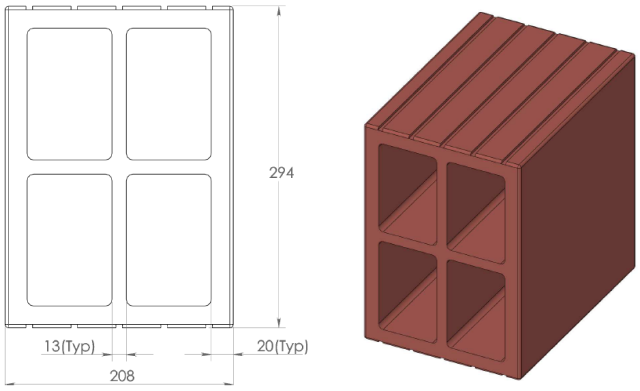

Figure 3: Measured dimensions of structural clay tile.

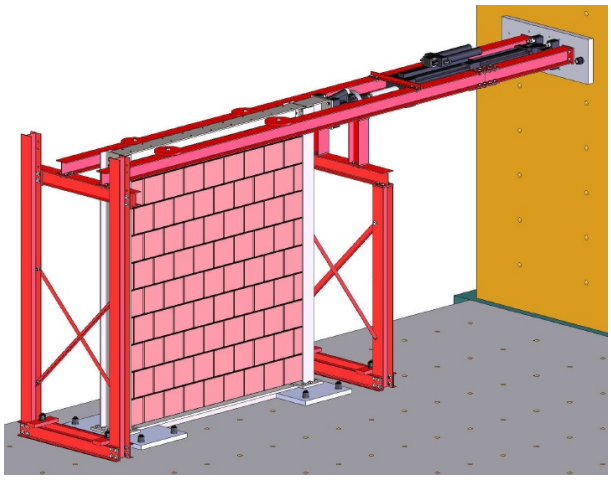

Figure 4: Experimental setup.

The experimental results showed that the type N mortar had a 17.69 MPa average compressive strength (C.O.V. 11 %), which exceed the required (ASTM C270) minimum compressive strength of 5.17 MPa [9]. Note that unlike concrete, mortar classification is based on formulation rather than compressive strength.

The characterization results are presented in Table 1, which lists compressive strength (based on gross area) and elastic modulus results of T, P and D tile specimens. The observed individual tile average compressive strength of 18.8 MPa largely exceeds the minimum of 4.8 MPa required by ASTM C34 [10]. For the two tiles and 4x4 tiles prisms, the observed compressive strength drops to 7.1 MPa and 2.0 MPa, respectively. The tested specimens show an average elastic modulus of 5 000 MPa, except in the case of the diagonal tests, where an average value of 6 800 MPa was observed and can be attributed to masonry anisotropy (the presence of mortar joints lead to

materiel anisotropy). Other properties for the structural clay tiles include their weight (14 kg), Poisson's ratio (0.14, C.O.V. 16 %) and density (813 kg/m³).

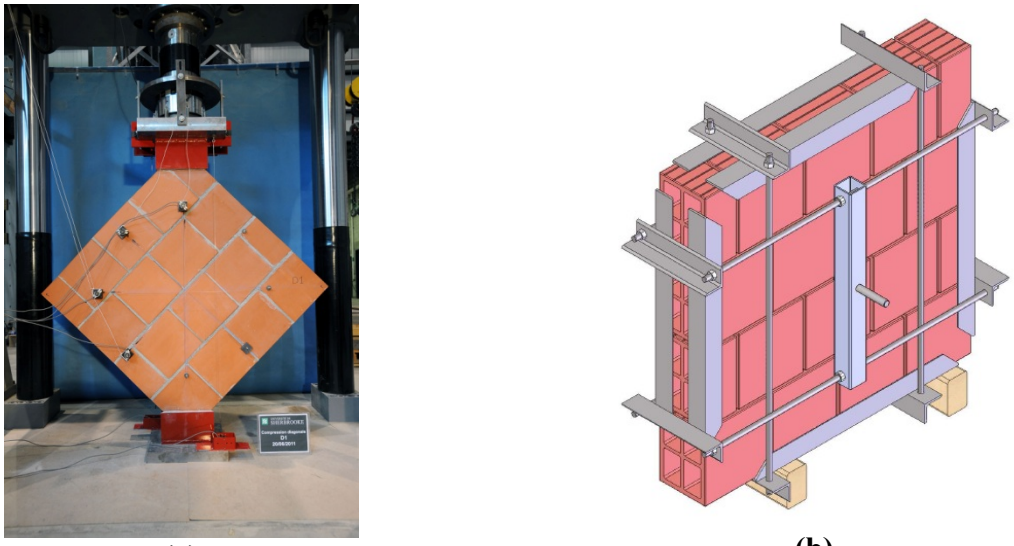

(a) (b)

Figure 5: 4x4 tiles prism: (a) diagonal compressive setup; (b) clamping system for manipulation.

Table 1: Characterization results of individual tiles and tiles assemblies.

Results / Specimen	Test Number	Compressive strength			Elastic modulus		
		Individual (MPa)	Average (MPa)	C.O.V. %	Individual (GPa)	Average (GPa)	C.O.V. %
T	1	14.02	18.8	16	4 300	4 940	13
	2	18.41			4 500		
	3	18.33			5 000		
	4	21.62			5 000		
	5	21.47			5 900		
P	1	7.40	7.1	3	4 700	4 967	11
	2	7.09			5 600		
	3	6.94			4 600		
D	1	2.13	2.0	15	6 900	6 833	35
	2	2.22			9 200		
	3	1.67			4 400		

Figure 6 shows stress-deformation curves of individual tiles and tiles assemblies where elastic behavior and fragile failure are observed. In the case of individual tile specimens, the failure is nearly explosive with spall projections at high velocity. Cracking is parallel to loading, first through horizontal internal web and then through horizontal faceshell. For two tiles prism specimens, the failure mode is very similar, but with less spalling. Cracking is also parallel to loading, but passing through the mortar joint and also through the vertical internal web of both tiles. In the case of 4x4 tiles prisms, cracking occurs in the mortar joints, with a stepped pattern, followed by the complete separation of the specimen at the mortar to masonry unit interface.

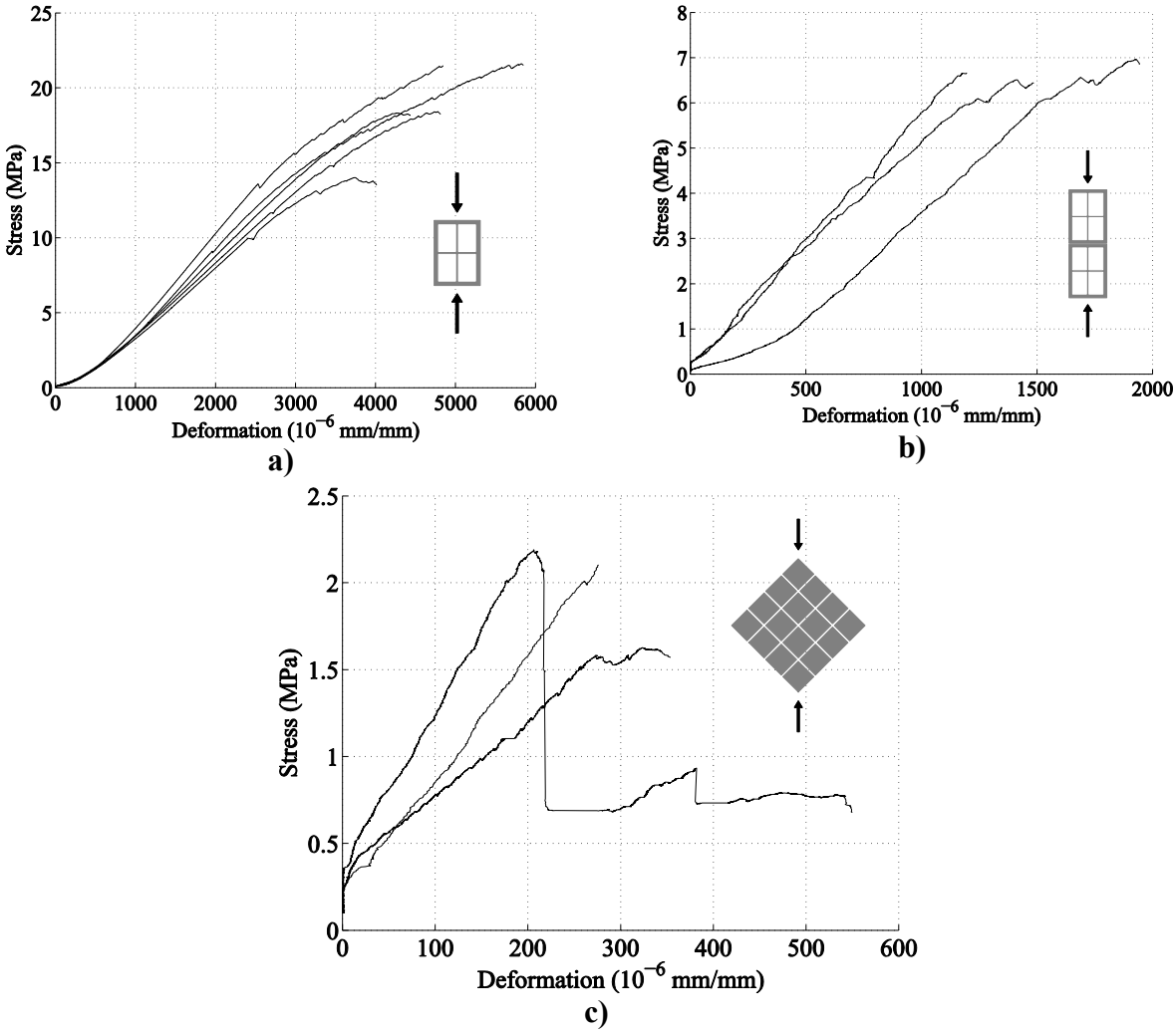

Figure 6: Stress-deformation curves: a) individual tile; b) two tiles prism; c) 4x4 tiles prism specimens.

IN-PLANE CYCLIC TEST RESULTS

Figure 7 shows the load-displacement curves resulting from the in-plane cyclic test. The hysteresis curves demonstrate an inelastic behavior typical of unreinforced masonry with pinched loops and strength degradation after peak response. The experimental specimen failed by a diagonal compressive mechanism with corner crushing. Note that the positive direction corresponds to the actuator pushing the specimen, while it is pulling in the negative direction.

Six stages are identified in Figure 7 and correspond to different behavior of the infill wall during testing. The first stage is a pure bending behavior where the steel frame and the masonry infill act as one element. The next stage, which happens early in the tests, is a separation between the masonry wall and the steel frame (a 3 mm lateral displacement is applied at this stage). The steel frame and the masonry wall deform differently, creating a frame-wall interaction. Cracking of mortar joints then occurs on wall diagonals, with a stairway pattern (5 mm displacement). Generally, cracking occurred at the tile interface, as was observed for the 4×4 tiles prisms. Stress

redistribution occurs with the enlargement of the cracked zones. The displacement reaches 8 to 12 mm when significant cracking occurs in the mortar joints and this is accompanied by cracking in the compressed tiles. The peak response corresponds to the first tiles failures under the beam and on the compressed diagonal (20 mm displacement). Finally, the specimen strength decreases with the fragile failure of more tiles (32 mm displacement). A final 36 mm lateral displacement was applied to investigate residual strength.

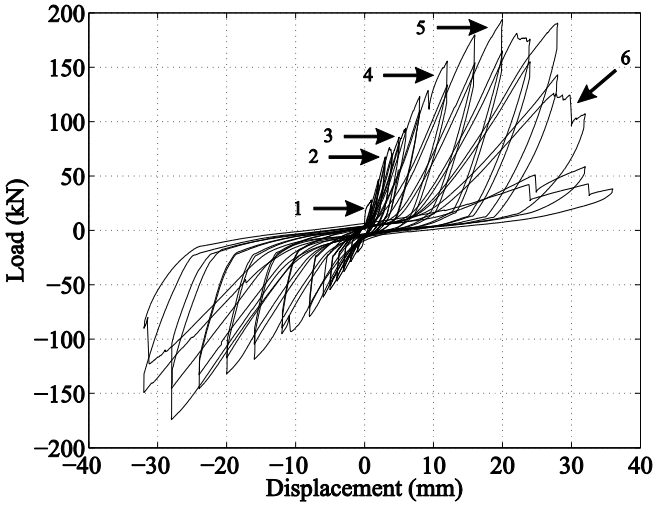

Stages

1. Pure bending
2. Beginning of frame-wall interaction
3. Beginning of diagonal cracking
4. Beginning of tile cracking
5. Peak load and tile failure
6. Wall failure with loss of tiles

Figure 7: Complete hysteresis of the in-plane cyclic test.

Figure 8 shows an indicator to investigate stiffness degradation during the cyclic tests. The normalized ratio of load, L, at target displacement to target displacement, D, (L/D), is plotted as a function of the target displacement. The 100 % value corresponds to the initial state of the wall, at a lateral displacement of 1 mm or less, and is equal to 28. kN/mm. The curve shows that there is a 50 % stiffness degradation at occurrence of cracking, and a 75 % degradation at peak response.

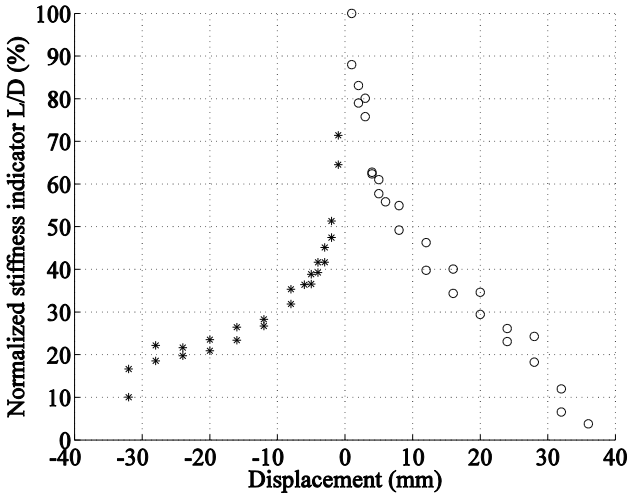

Figure 8: Stiffness degradation of experimental specimen.

Figure 8 also shows that for each displacement cycle, the observed stiffness was 35 % less in the negative (pull) direction than in the positive (push) direction. An average stiffness degradation of 12 % was observed for each cycle repetition. The stiffness decrease varies according to the displacement, and therefore to the damage type. When separation is initiated between the masonry wall and the steel frame, the stiffness indicator decreases by 5 % with cycle repetition. This degradation is more important for mortar joints cracking and for tile failure, with an average decrease of 12 % and 32 %, respectively.

The experimental specimen had a peak response of 194 kN, corresponding to a 20 mm lateral applied displacement. At the occurrence of diagonal cracking (5 mm displacement), the specimen had reached 30 % of its maximum capacity. As tiles began to fail after the peak response (32 mm displacement), the specimen was at 80 % of its maximum capacity. At the end of the test (36 mm displacement), the specimen had a residual capacity of 20 %.

Contrary to observed behavior of the 4×4 tile prism used in the characterization phase, where cracking apparition corresponded to the maximum strength and subsequent failure of the specimens, the failure of the infill wall did not occur immediately after diagonal cracking had begun. The peak response of the infill wall was approximately three times larger than the strength at the onset of cracking. This seems to indicate that the frame confined the masonry and this prevents fragile failure when cracking occurs, a consequence of the interaction between the frame and the wall.

In the context of seismic performance, the damage state is often linked with deformation. The cracking was first observed at a lateral drift of 0.16 %, while the peak response occurred at a lateral drift of 0.67 %. At a drift of 1.07 %, the wall was at 80 % of its maximum resistance.

Figure 9 shows a bilinear idealization of the hysteresis envelope. The first part of this idealization accounts for the development of compressive diagonal mechanism, and the plateau accounts for the stability of the maximum strength until wall failure at a displacement of 32 mm. The slope of the first part was determined so that the area under the curve was equal up to maximum response. The intersection of both lines occurs at a displacement of 13.64 mm. Considering this displacement as the equivalent yield point, the equivalent ductility of the wall is 32/13.64 = 2.5.

The energy dissipated by the wall can be evaluated using the internal area of the hysteresis loops. The wall was subjected to a total of 25 loading cycles and dissipated a total of 19 746 kNmm. Figure 10 presents a graph of the energy dissipated as a function of the target displacement.

Energy dissipation increased with the target displacement until a value of 28 mm, where there were many compressive tile failures. The energy dissipation was 20-25 % higher in the positive (push) direction than in the negative (pull) direction. Also, there was generally 30 % less energy dissipation with cycle repetition.

NUMERICAL ANALYSIS

Numerical analyses were carried out using the masonry element of the SeismoStruct program [11]. This four node element was developed by Crisafulli [12] to analyse in-plane behavior of

frames with infill masonry walls. The macro-model is based on the equivalent strut concept with hysteresis rules for cyclic nonlinear compressive and shear behaviours. The geometry of the masonry element and its behavior are described by thirty parameters.

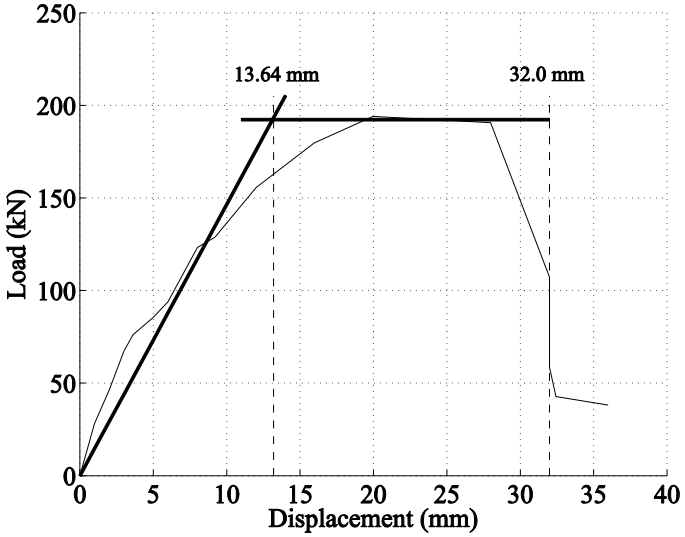

Figure 9: Bilinear idealized hysteresis envelope.

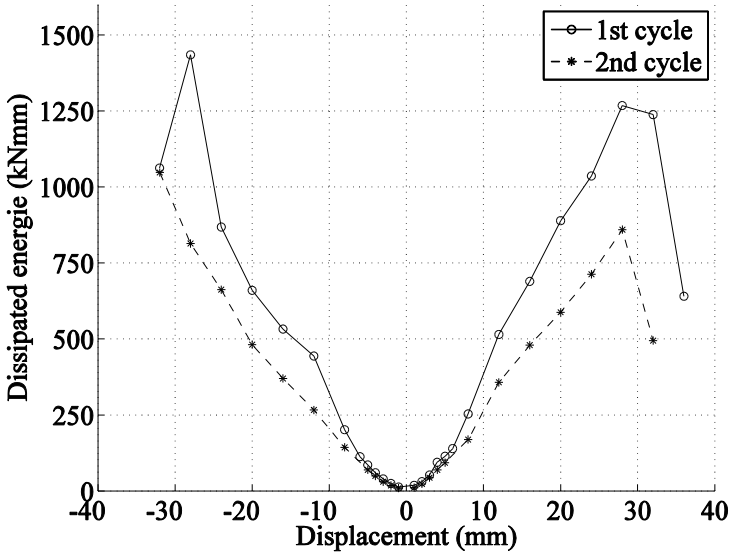

Figure 10: Dissipated energy by displacement direction, for each cycle.

Ten adaptive pushover analyses were carried out to compare the numerical prediction with experimental results. Key parameters were varied (especially those related to geometry and compressive behavior) using the masonry characterization results as a basis, as well as a rational methodology based on the masonry element formulation. The masonry characterization tests yielded compressive strengths (2.0 MPa), elastic modulus (5 000 MPa) and deformation at maximum stress (0.00025 mm/mm).

Figure 11 shows the numerical results of four models and the positive envelope of the experimental hysteresis. The strut area used in the model were selected according to Mainstone [13] (C1b in Figure 11; 0.07 m²), Liauw and Kwan [14] (C2b; 0.13 m²), Decanini and Fantin [15] (C3b; 0.14 m²) and Paulay and Priestley [16] (C4b; 0.20 m²). The work of Decanini and Fantin on cracked state was also considered with a strut area modification factor after cracking (54 %) which was similar to experimental results.

Figure 11 shows that the numerical models overestimate the infill wall initial stiffness by a factor ranging between 1.6 and 2.5. The C1b model leads to a better initial stiffness prediction. The same model also yields the best load capacity approximation, whereas models C2b to C4b overestimate this value by a factor of 1.8. All numerical models, however, underestimate the residual capacity of the infill wall, except for C4b model that results in a different failure mode. In the case of predicted deformation, the numerical predictions largely vary, particularly for the C2b and C3b models that nearly have the same parameter values. But it is also interesting to note that the C3b model give a relatively good approximation for displacements. As for dissipated energy, only the C1b model has approximately the same area under the capacity curve.

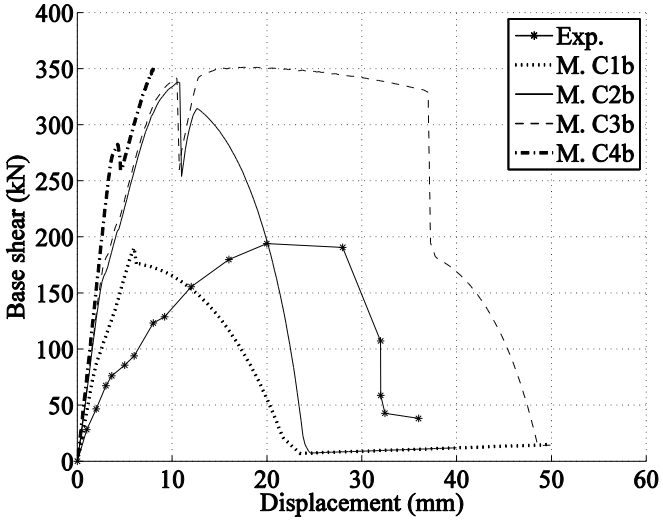

Figure 11: Numerical capacity curves compared with experimental results.

Models C1b and C3b were found to give the most interesting predictions, but the large number of parameters and limited number of characterization values made it difficult to further optimize the models.

CONCLUSION

The experimental program on structural clay tile, a material that was widely used in a large number of school buildings in Quebec, yielded key information on the dynamic behavior of this type of material. Tests showed that, even in the case of non-structural URM infills, there is clearly interaction with the structural frame during cyclic loading. Contrary to compressive characterization tests results, the experimental infill wall specimen demonstrated load-bearing capacity after diagonal cracking. A numerical correlation study carried out with a specialized masonry element yielded interesting predictions when compared to experimental results, but also

showed the challenge of selecting the adequate modelling parameters. The experimental data obtained in this project, coupled with the results from an ongoing in-situ ambient vibration measurement investigation, could be used in a seismic safety evaluation study for steel and concrete frames school buildings with structural clay tiles.

ACKNOWLEDGEMENTS

Support from Canadian Seismic Research Network (a NSERC Strategic Network) as well as from the Fonds de recherche du Québec – Nature et technologies (FRQNT) is acknowledged. The authors would like to thank Louis-Gabriel Paquette (Exp, Drummondville, QC) as well as the technical staff at the Université de Sherbrooke structural laboratory.

REFERENCES

1. Canadian Seismic Research Network (CSRN), http://csrn.mcgill.ca/main.html.
2. Therrien-Truchon, J. (2012) "Seismic Behavior of Structural Clay Tiles Infill Masonry Walls" Master Thesis (*In French*), Université de Sherbrooke, Sherbrooke, Quebec, Canada.
3. Paquette, L.-G. (2012) "Characterization of buildings with unreinforced masonry and their dynamic properties" Master Thesis (*In French*), Université de Sherbrooke, Sherbrooke, Quebec, Canada.
4. ASTM (2008) "C109 Standard Test Method for Compressive Strength of Hydraulic Cement Mortars (Using 2 in. or 50 mm Cube Specimens)".
5. ASTM (2009) "C67 Standard Test Methods for Sampling and Testing Brick and Structural Clay Tile".
6. ASTM (2010) "C1314 Standard Test Method for Compressive Strength of Masonry Prisms".
7. ASTM (2010) "E519 Standard Test Method for Diagonal Tension (Shear) in Masonry Assemblages".
8. ASTM (2009) "C1552 Standard Practice for Capping Concrete Masonry Units, Related Units and Masonry Prisms for Compression Testing".
9. ASTM (2010) "C270 Standard Specification for Mortar for Unit Masonry".
10. ASTM (2003) "C34 Standard Specification for Structural Clay Loadbearing Wall Tile".
11. SeismoSoft (2006) SeismoStruct – A Computer Program for Static and Dynamic Nonlinear Analysis of Framed Structures.
12. Crisafulli, F. J. And Carr, A. J. (2007) "Proposed Macro-Model for the Analysis of Infilled Frame Structures" Bulletin of the New-Zealand Society for Earthquake Engineering, Volume 40, Issue 2.
13. Mainstone, R. J. (1971) "On the Stiffnesses and Strengths of Infilled Frames" Supplement IV of Proceedings of the Institution of Civil Engineering. Number 7360S.
14. Liauw, T.-C. and Kwan, K.-H. (1984) "Nonlinear Behavior of Non-Integral Infilled Frames" Computers and Structures, Volume 18, Issue 3.
15. Decanini, L. D. and Fantin, G. E. (1986) "*Modelos simplificados de la mampostería incluida en pórticos. Características de rigidez y resistencia lateral en estado límite*" (*in Spanish*), Jornadas Argentinas de Ingeniería Estructural, Volume 2.
16. Paulay, T. and Priestley, M. J. N. (1992) "Seismic Design of Reinforced Concrete and Masonry Buildings" John Wiley & Sons, Inc.